Journal of Photochemistry and Photobiology A: Chemistry 217 (2011) 425–429

Contents lists available at ScienceDirect

Journal of Photochemistry and Photobiology A: Chemistry

journal homepage: www.elsevier.com/locate/jphotochem

Research of photocatalytic degradation of HeLa cells at the TiO_2 interface by ATR-FTIR and fluorescence microscopy

E. Kabachkov*, E. Kurkin, V. Nadtochenko, A. Terentyev

Institute of Problems of Chemical Physics of RAS, Acad. Semenov Av., 1, Moscow Region, Chernogolovka 142432, Russian Federation

ARTICLE INFO

Article history:
Received 10 August 2010
Received in revised form 1 November 2010
Accepted 25 November 2010
Available online 2 December 2010

Keywords:
Photocatalytic degradation
Cancer cells
TiO_2

ABSTRACT

Fourier Transform Infrared (FTIR) spectroscopy of Attenuated Total Reflection (ATR) and luminescence microscopy methods were applied to study oxidation kinetics for biomolecular components of eukaryotic HeLa cancer cells caused by photogenerated charges in TiO_2. It was shown, that organic matter of cells is mineralized on porous film of TiO_2 nanoparticles in such a way that TiO_2 surface does not show HeLa cell residues. Basic precursor organic groups Amide I, Amide II and phosphate are oxidized with different rates. Amide II is oxidizing with the highest rate, it is followed by Amide I, and phosphate is the most resistant to oxidation.

1. Introduction

Photocatalytic inactivation of eukaryotic cells placed on TiO_2 was studied previously on several occasions [1–8], but the process mechanism leading to photocatalytic destruction of animal cells still remains to be an object of thorough investigation. Investigations in this area are important for medicine, ecology, pharmaceutics, food industry, perfumery and for human health. The purpose of this work is to study photocatalytic destruction of HeLa line cancer cells with the use of nanocrystalline TiO_2 using method of Fourier Transform Infrared spectroscopy of Multiple Attenuated Total Reflection (FTIR-MATR). FTIR-MATR spectroscopy is used to resolve absorption bands of various biomacromolecules and products of photocatalytic oxidation. So, this approach allows us to identify the oxidation kinetics of separate cellular molecules and to determine important features of the mechanism of photocatalytic destruction of an animal cell located on mesoporous film of titanium dioxide.

2. Materials and methods

2.1. Materials

TiO_2 Hombifine N (320 m^2/g, 100% anatase) produced by Sachtleben Chemie GmbH was used as photocatalyst in all experiments.

Investigations were carried on for cancer cells of epithelioid carcinoma of human cervix uteri, HeLasubline. Culture conditions: DMEM medium, 10% fetal bovine serum, 37 °C, and 5% CO_2.

2.2. Preparation of mesoporous TiO_2 films

TiO_2 Hombifine N powder was used to prepare acidic aqueous suspension with TiO_2 content of 100 g/l. Using spreading rod, this suspension was uniformly applied to Superfrost Plus Heinz Herenz high adhesive capacity microscope specimen glass. The films were air dried for 1.5 h. Detailed structure of porous TiO_2 films was studied using Carl Zeiss Supra 25 scanning electron microscope.

2.3. Irradiation methods

Samples were irradiated in Axio Imager A1 optical microscope with HBO 103 W/2 OSRAM high-pressure mercury lamp and Carl Zeiss interference filter (Filter Set No. 02) with transmission maximum at $\lambda = 365$ nm. Luminous flux was determined using Aktakom ATT-1515 UV-radiometer, and it was about 210 mW/cm^2. Samples were irradiated in air with the protection of HeLa cells from drying out in physiological saline. At the same time, the samples were photographed using compact digital camera of Canon G10 microscope.

2.4. Control experiments

Porous Al_2O_3 films were prepared using plasmachemical ultrafine Al_2O_3 ($F_{spec.} = 72.7$ m^2/g, $d = 20.8$ nm, $\delta + \gamma$ phases), produced in microwave discharge air plasma in the same manner as TiO_2-films. They were used in control experiments instead of TiO_2.

* Corresponding author. Tel.: +7 4965227774.
E-mail address: evgen.ken@mail.ru (E. Kabachkov).

1010-6030/$ – see front matter © 2010 Elsevier B.V. All rights reserved.
doi:10.1016/j.jphotochem.2010.11.019

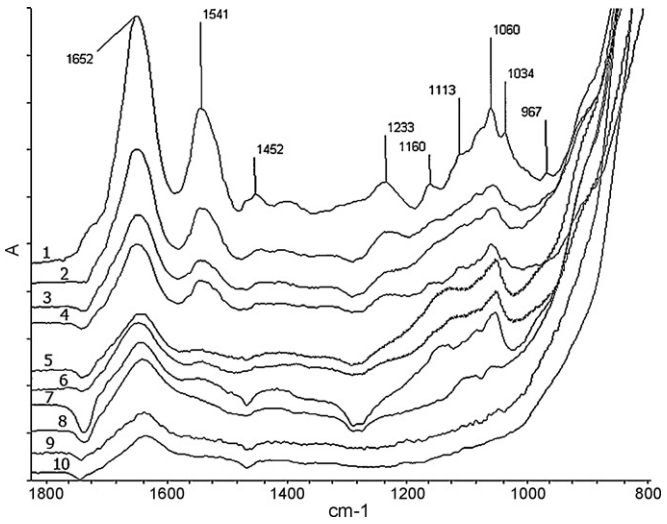

Fig. 1. Normalized FTIR-MATR spectra of HeLa cells on TiO_2 films after different times of light irradiation using HBO 103 W/2. Spectra of dry samples. Bands in the spectral region 1800–800 cm^{-1}. The integral absorbance in the region of 1800–800 cm^{-1} was used as the normalization factor. Exposure time: 0 (1), 3 (2), 4 (3), 6 (4), 8 (5), 14 (6), 20 (7), 60 (8), and 100 (9) min, (10) original TiO_2.

2.5. FTIR-MATR spectroscopy

Infrared spectra were determined using Perkin Elmer Spectrum 100 spectrometer with UATR add-on (Ge/KBr beam splitter). Spectrum data were accumulated using 10 scans with 4 cm^{-1} resolution in the range of 4000–675 cm^{-1}. Fourier deconvolution and second derivative of spectra were used to identify and evaluate FTIR-MATR spectral peaks. Fourier deconvolution and subtraction of spectra were performed using software package Peak Fit v4.12. Peak profiles were described using adjustable Gaussian or Lorentzian function in Wave Metrics Igor Pro v6.1.1 program. Peaks position error was limited by reproducibility of sample preparation and mechanical contact between the sample and UATR crystal.

2.6. Preparation of samples for FTIR-MATR spectroscopy

HeLa cells applied onto porous TiO_2 films in form of aqueous suspension with the concentration of 3×10^6 cells/ml. To provide reproducibility of measurements, porous TiO_2 films with uniform layer of HeLa cells were cut into separate parts. These TiO_2 parts were exposed to UV-A radiation for different time intervals. Films of plasmachemical ultrafine Al_2O_3 powder not featuring photocatalytic activity were used for control experiments.

Samples for fluorescence microscopy were prepared in a similar manner with the addition of 0.05 ml ethidium bromide of 10 mg/ml concentration into the HeLa cell suspension being applied, thus DNA of nonviable cells became purple colored. Discoloration of cells was used to plot a plasma membrane destruction curve.

3. Results and discussion

3.1. FTIR-MATR spectra of HeLa cells on TiO_2 Hombifine N films

FTIR-MATR spectra of HeLa cells on TiO_2 films are shown in Fig. 1. Spectral band assignment is given in Table 1.

3.2. Spectrum of pure TiO_2 film

This spectrum shows the following characteristic properties: steep shoulder up to 1000 cm^{-1}, caused by TiO_2 lattice vibrations, 1640 cm^{-1} band of approximately 100 cm^{-1} width, caused by water adsorbed on TiO_2 surface, broad peak in the area of 3600–2800 cm^{-1} with maximum at 3263 cm^{-1} –O–H vibrations of adsorbed water [9].

Table 1
Assignment of the FTIR-MATR bands of HeLa cells deposited on TiO_2 porous film [9–13].

cm^{-1}	Assignment	cm^{-1}	Assignment
3281	Amide A	1395	$-COO^-$ str.
3072	Amide B	1233	Amide III
2965	$\nu_a(CH_3)$	1160	ν(C–O) ring
2920	$\nu_a(CH_2)$	1113	ν(C–O)
2876	$\nu_s(CH_3)$	1085	$\nu_s(PO_{2-})$
1652	Amide I	1060	P–OR ester
1541	Amide II	1034	δ(C–OH) of carbohydrates
1452	$\delta_a(CH_3)$	967	C–N stretching asymmetric

Evolution of FTIR-MATR spectra associated with destruction of HeLa cells and caused by photocatalytic oxidation of cellular molecules on TiO_2, is shown in Fig. 1 in spectral region of characteristic IR-bands. Spectra in Fig. 1 were normalized to provide the comparison of changes by one and the same scale, for this purpose spectra in the range of 800–1800 cm^{-1} were divided by the value of spectral integral, calculated for this spectral range. Spectral integral is calculated as

$$I(\nu) = \int_{\nu_0}^{\nu_1} \frac{S(\nu)d\nu}{\nu}$$

where $S(\nu)$ – FTIR-MATR spectrum recorded by the device.

Spectra in Fig. 1 show significant changes in spectrum profile of original shape of HeLa cell bands already in 3 min after starting the UV-irradiation. Asymmetric methyl protein group bands near 1452 cm^{-1} and C–O modes of C–OH serine, threonine and tyrosine groups in cell proteins near 1160 cm^{-1} [10] disappear. Weak bands at 1113, 1034 and 967 cm^{-1} disappear as well. Phosphor-ester peak P–OR near 1060 cm^{-1} is drastically smoothed and decreased. This gives evidence of the quick destruction of HeLa cell membrane, since phosphor-ester peak is created largely due to strong absorption in external phospholipid bilayer [11]. Amide bands, II – 1541 cm^{-1} and III – 1233 cm^{-1}, disappear after 8 min of UV-irradiation. At the same time, a broad band of –C–OH valence vibrations appears at 1190–1120 cm^{-1}, and this is indicative of the increased concentration of hydroxyl groups. Amide I peak at 1652 cm^{-1}, for the most part caused by macromolecular components of HeLa cell nucleus [11], is smoothed rather quickly, but remains to be one of the most appreciable peaks. Approximately 100 min of UV-irradiation on TiO_2 is required for its full disappearance.

Fig. 2 shows FTIR-MATR spectra of HeLa cells on TiO_2 films, obtained by the deconvolution of experimental FTIR-MATR spectra. Deconvolution made it possible to resolve separate peaks in Amide I band near 1652 cm^{-1}: at 1655 cm^{-1} and two secondary peaks at 1685 and 1636 cm^{-1}, which correspond to different structural conformations of protein macromolecules [12]. As the diagram shows, relative intensities of three Amide I peaks at 1685, 1655 and 1636 cm^{-1}, as well as intensities of two Amide II peaks at 1545 and 1519 cm^{-1} are decreased already after 5 min of UV-irradiation. This shows that secondary protein structures in HeLa cells are changed under the influence of photocatalytic oxidation. At the second, peaks in the range of 1160–950 cm^{-1} were resolved. They pertain mainly to carbohydrate and oligosaccharide bands (1156, 1131, 1111, 1029, and 1006 cm^{-1}) [10], phosphate bands PO_2^- (1085 cm^{-1}) [12] and phosphor-ester band (1060 cm^{-1}). These band shapes are drastically changed after 5 min of irradiation, which implies, most probably, the destruction of cellular plasma membrane, occurring during photocatalysis.

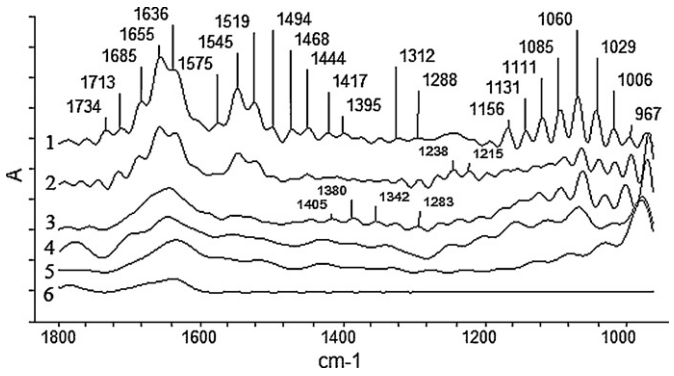

Fig. 2. Fourier deconvoluted spectra of HeLa cells from 1800 to 950 cm^{-1} after different irradiation times on the TiO_2 films interface. Exposure time: 0 (1), 5 (2), 15 (3), 30 (4), 60 (5), and 100 (6) min. Deconvolution parameters: FWHM = 21.945 and a frequency filter data F = 67% with a linear basis.

For comparison, Fig. 3 shows also the results of control experiments, where HeLa cell suspension was applied onto porous Al_2O_3 film. FTIR-MATR spectrum of this system does not show significant changes after 100 min of UV-irradiation. Only small deviations appear in the shape of Amide I and Amide II bands. Inspection results conclusively establish photocatalytic nature of the oxidation of HeLa cell substrates on the surface of nanocrystalline TiO_2 and minor change of cell spectrum under UV-A-irradiation on Al_2O_3 film.

3.3. Kinetics of FTIR-MATR spectra of HeLa cells during photocatalytic oxidation

Decrease in integral intensity of FTIR-MATR spectral bands implies mineralization of organic matter on the TiO_2 surface during photocatalysis. The kinetics of integral absorption is only a rough approximation for the evaluation of the amount of organic matter on the TiO_2, because the molar absorption coefficients are different for various intermediate products of photocatalytic oxidation. Nevertheless, the integral absorption in broad spectral region is proportional to the sum of organic matter assuming that the integral of IR transitions oscillators' strengths remains approximately constant. Value of spectral integral was calculated in the range of 1800–950 cm^{-1}. Kinetics of integral absorption of HeLa cells is shown in Fig. 4. Experimental data can be approximated by exponential curve, which describes the decomposition kinetics of organic matter of HeLa cells. The curve does not show the survival kinetics since it is obvious that all cells loose their viability shortly after starting irradiation because of UV-induced damages;

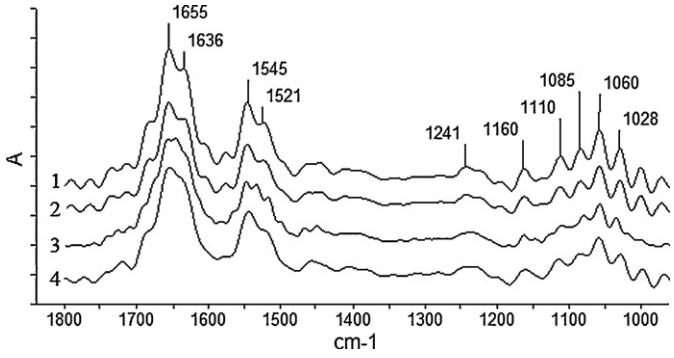

Fig. 3. Fourier deconvoluted spectra of HeLa cells from 1800 to 950 cm^{-1} after different irradiation times on the Al_2O_3 films interface. Exposure time: 0 (1), 20 (2), 40 (3), and 100 (4) min. Deconvolution parameters: FWHM = 21.945 and a frequency filter data F = 67% with a linear basis.

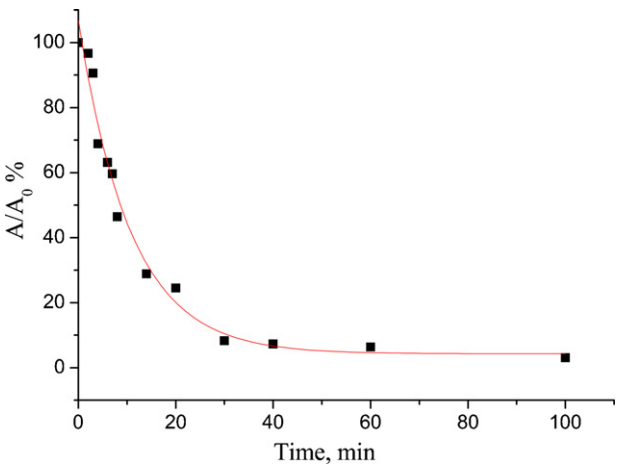

Fig. 4. Kinetics of FTIR-MATR spectra of HeLa cells in the range of 1800–950 cm^{-1} during photocatalytic oxidation on the TiO_2 surface.

and all cells die during irradiation on both Al_2O_3 and TiO_2 films. The kinetics observed demonstrates the photocatalytic destruction of cellular substances in all cells, both alive at the beginning of experiment and killed in the course of irradiation. Decomposition rate constant equals to $(9.3 \pm 0.1) \times 10^{-2}$ min^{-1}. After 30 min of UV-irradiation, the integral of absorption spectrum is less than 10% of initial FTIR-MATR spectrum. This is indicative of low resistance of macromolecular components of eukaryotic HeLa cell to photocatalytic oxidation.

As it was noted above, increase in intermediate destruction products bands is observed simultaneously with decrease in original bands in the HeLa spectrum. Because of overlapping of various bands, accurate resolution into separate peaks is impossible when unconstrained minimization procedures are used. Nevertheless, it is possible to derive an approximate evaluation of the integral absorption of the separate bands as a function of reaction time.

Fig. 5 shows the dynamics of integral absorption variation in the peaks Amide I at 1700–1586 cm^{-1}, Amide II at 1580–1478 cm^{-1} and in the phosphate PO_2^- band at 1135–1010 cm^{-1}. These spectral bands present two components a high degradation rate and a slower one. Quick stage lasts for about 10 min and is likely to be associated with the destruction of plasma membrane of HeLa cells. Exponential-function approximation gives decomposition rate constants: $(12.6 \pm 0.1) \times 10^{-2}$ min^{-1} for

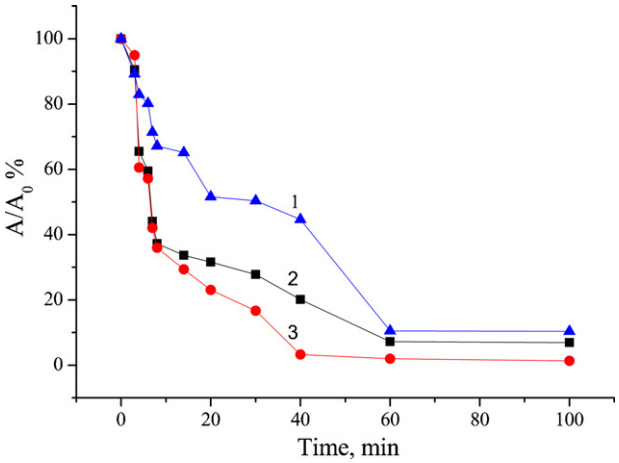

Fig. 5. Kinetics of the decay ratio of the absorbance areas. 1 – phosphate PO_2^- band region 1135–1010 cm^{-1}, 2 – Amide I band region 1700–1586 cm^{-1}, and 3 – Amide II band region 1580–1478 cm^{-1} of HeLa cells.

Amide I band, $(13.3 \pm 1.2) \times 10^{-2}\,min^{-1}$ for Amide II band and $(4.8 \pm 0.2) \times 10^{-2}\,min^{-1}$ for PO_2^- band. Amide II band disappears with the highest rate, which is indicative of the quick destruction of NH-bonds in HeLa cell proteins. Second slow stage lasts for 10–40 min for Amide II band with the constant equal to $(8.0 \pm 1.1) \times 10^{-2}\,min^{-1}$. For Amide I and PO_2^- bands, it lasts for 10–60 min, with constants, correspondingly $(3.4 \pm 0.2) \times 10^{-2}\,min^{-1}$ and $(3.7 \pm 0.6) \times 10^{-2}\,min^{-1}$.

Oxidation rate of macromolecules including Amide I, Amide II and PO_2^- bands qualitatively correlates with bond energies in accordance with Semenov/Polanyi theory: the highest oxidation rate has N–H bond (348 kJ/mol), other bonds require more energy for breaking: 653 kJ/mol for C=O and 419 kJ/mol to break away phosphate. Besides, it should be taken into account, that kinetic absorption curve of phosphate band 1135–1010 cm^{-1} is distorted by slowing-down in the interval of 30–40 min, due to the overlapping of absorption bands of intermediate products of photocatalytic oxidation [13].

3.4. Loss of plasma membrane integrity of HeLa cells at photocatalysis

Plasma membrane integrity can be demonstrated with use of membrane impermeable compounds that do not enter cells with intact membrane. As a marker of plasma membrane integrity, we used DNA intercalating agent ethidium bromide that binds to DNA of cells with damaged plasma membrane and does not stain DNA in intact cells. As it is seen on Fig. 6, under UV-A irradiation on the surface of mesoporous TiO_2 photocatalyst films cells loose their membrane integrity very quickly compared to Al_2O_3 films. Ultraviolet as such induces cell death, but this cellular response is the well-known process of programmed cell death (apoptosis) in which it takes at least several hours to cause notable cell membrane permeabilisation, as it was demonstrated in experiments with UV irradiation at doses close to used in our work [20,21]. Unlike slow cellular response on UV-A irradiation Al_2O_3 films, photocatalytically created peroxy radicals on TiO_2 films cause fast destruction of plasma membrane of cells.

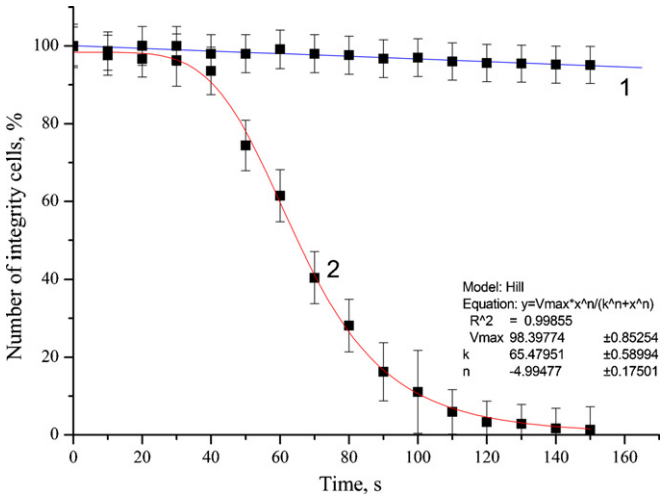

Fig. 6. Integrity of HeLa cells on the Al_2O_3 (1) and TiO_2 (2) films interface at UV-A irradiation. Experimental data are approximated by generalized Hill functions.

Point of interest in curve 2 presented in Fig. 6 is the presence of two phases of cell protection states. The first phase lasting for about 40 s, as noted in the literature [14], is associated with operation levels of life sustaining systems. Drastic fall of living HeLa cells' fraction after 40 s means a drastic change of host defenses–transition into a new state resulting in host death in accordance with the theory of oxidative stress [14–16]. Experimental data are well approximated by generalized Hill functions frequently used for simulating of bacterial cell metabolism and for construction of universal "electronic

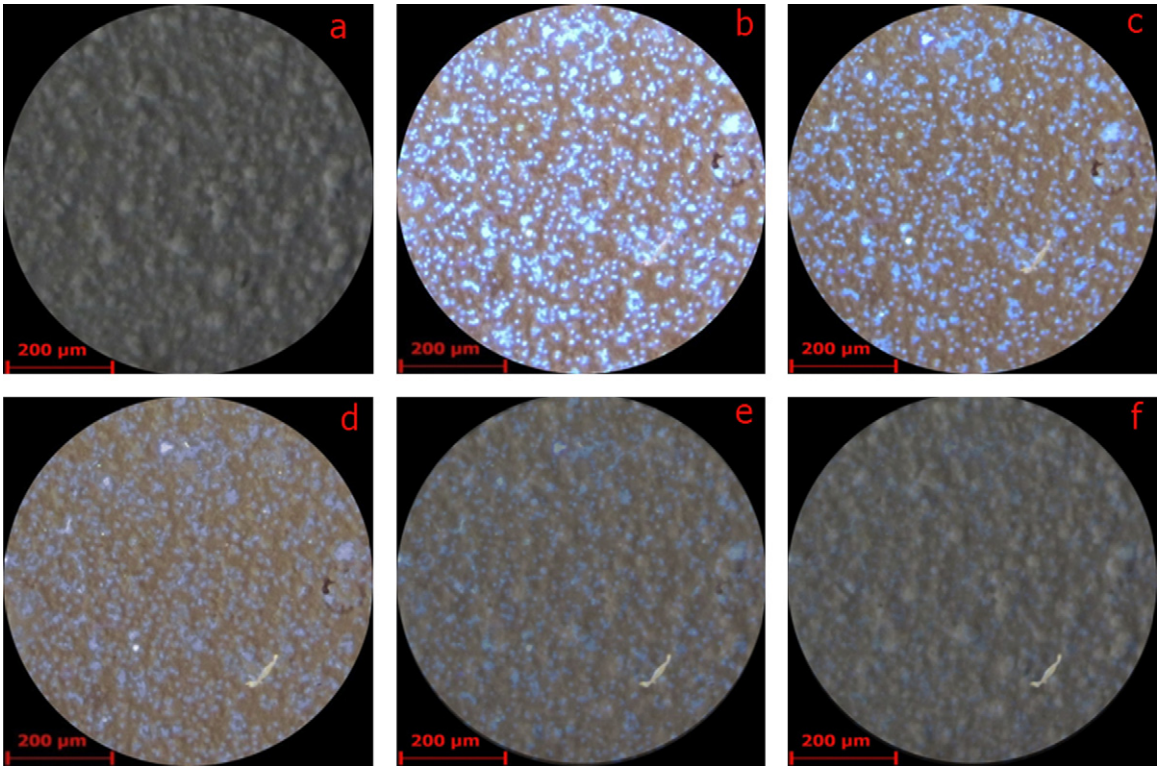

Fig. 7. Photomicrographs of HeLa cells before and during UV-A irradiation on the TiO_2 surface. Exposure time: (a) original TiO_2, (b) HeLa cells on the TiO_2 surface 0 min, (c) 5 min, (d) 30 min, (e) 60 min, and (f) 100 min.

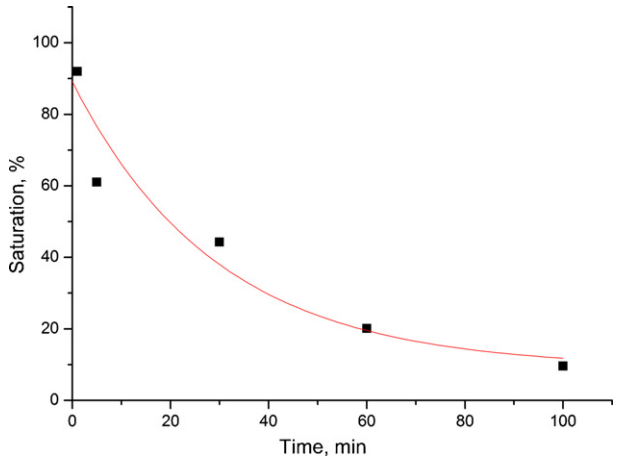

Fig. 8. HeLa cells' luminescence saturation of RGB spectrum blue channel versus UV-irradiation time on the TiO_2 surface.

cell" [17]:

$$f(x) = d \cdot V_{\max}, \quad d = \frac{x^n}{k^n + x^n},$$

where $f(x)$ is logistic function, d is fraction of occupied sites, $V_{\max}$ is maximum amount $f(x)$, x is time, k is apparent dissociation constant, and n is the Hill coefficient.

HeLa cells on the surface of mesoporous TiO_2 films loose their membrane integrity in the first 1–2 min after starting UV-A irradiation. At a later time, only photocatalytic destruction of organic matter of dead cells and self-cleaning of photocatalyst surface take place.

3.5. Mineralization of killed HeLa cells at photocatalysis

For the confirmation of surface self-cleaning, photomicrographs of HeLa cells before and during UV-A irradiation are presented in Fig. 7. Under irradiation with 365 nm wavelength light, HeLa cells have intensive blue color, associated with proteins composing its basis, reduced pyridine nucleotides (NADH and NADPH) and oxidated flavoproteins (flavine mononucleotide and flavine adenine dinucleotide) [18,19]. In the same manner as in the case of FTIR-MATR spectra of HeLa cells noticeable changes occur already after 5 min from starting irradiation (Fig. 7b and c). After 100 min of photocatalytic oxidation of dead cells, nanocrystalline TiO_2 practically completely destroys HeLa cells, and the photocatalyst surface recovers its original appearance (Fig. 7f and a). Fig. 8 shows the saturation of RGB spectrum blue channel versus UV-irradiation time behavior. In color theory, saturation is intensity of certain tone that is the degree of visual difference between chromatic color and achromatic (grey) color of equal brightness. Variation of HeLa cells' luminescence saturation can be approximated by exponential curve. According to general idea, curve and the saturation should be proportional to the total sum of organic matter. On this assumption, calculated decomposition rate constant equals to $(3.3 \pm 0.2) \times 10^{-2}\ \mathrm{min}^{-1}$, which is slightly below the rate constant ($(9.3 \pm 0.1) \times 10^{-2}\ \mathrm{min}^{-1}$), calculated based on integral absorption in FTIR-MATR spectra of HeLa cells for the region of 1800–950 cm^{-1}. At the same time, fluorescence microscopy confirms FTIR-MATR data on deep photocatalytic oxidation of HeLa cancer cells on the surface of nanocrystalline titanium dioxide.

4. Conclusions

By means of Fourier Transform Infrared spectroscopy and fluorescence microscopy methods it was shown that organic matter of eukaryotic HeLa cells is photocatalytically oxidated on the surface of porous TiO_2 film under irradiation by light with $\lambda = 365$ nm and luminous flux density about 210 $\mathrm{mW/cm}^2$. The surface of nanocrystalline TiO_2 photocatalyst can degrade cancer cells intermediate products at long-term UV irradiation. Photocatalytic oxidation of basic organic groups Amide I, Amide II and phosphate on TiO_2 surface occurs at different rates. Amide II is being oxidized with the highest rate, it is followed by Amide I, and phosphate is the most resistant to photocatalytic oxidation.

References

[1] R. Cai, K. Hashimoto, K. Itoh, Y. Kubota, A. Fujishima, Bull. Chem. Soc. Jpn. 64 (1991) 1268–1273.
[2] D.M. Blake, P.-C. Maness, Z. Huang, E.J. Wolfrum, J. Huang, W.A. Jacoby, Sep. Purif. Methods 28 (1) (1999) 1–50.
[3] M. Kalbacova, J.M. Macak, F. Schmidt-Stein, C.T. Mierke, P. Schmuki, Phys. Stat. Sol. (RRL) 2 (4) (2008) 194–196.
[4] P. Thevenot, J. Cho, D. Wavhal, R.B. Timmons, L. Tang, Nanomedicine 4 (September (3)) (2008) 226–236.
[5] A.-P. Zhang, Y.-P. Sun, World J. Gastroenterol. 10 (November (21)) (2004) 3191–3193.
[6] L. Liua, P. Miaoa, Y. Xua, Z. Tianb, Z. Zoub, G. Li, J. Photochem. Photobiol. B: Biol. 98 (March (3)) (2010) 207–210.
[7] Y. Sun, J. Xu, W.-B. Cai, Z.-Y. Jiang, Acta Phys. Chim. Sin. 24 (2008) 1359–1365.
[8] A. Fujishimaa, X. Zhangb, D.A. Trykc, Surf. Sci. Rep. 63 (December (12)) (2008) 515–582.
[9] M. Primet, P. Pichat, M.V. Mathieu, J. Phys. Chem. (75) (1971) 1216.
[10] P.T. Wong, R.K. Wong, A. Thomas, Biochemistry 88 (1991) 10988–10992.
[11] M. Miljkovic, M. Romeo, C. Matthäus, M. Diem, Biopolymers 74 (May (1–2)) (2004) 172–175.
[12] V.A. Nadtochenko, O.M. Sarkisov, V.V. Nikandrov, P.A. Chubukov, N.H. Denisov, Chem. Phys. 27 (1) (2008) 26–36.
[13] J. Kiwi, V. Nadtochenko, Langmuir (21) (2005) 4631–4641.
[14] A.I. Michalski, T.E. Johnson, J.R. Cypser, A.I. Yashin, Biogerontology 2 (2001) 35–44.
[15] D. Harman, J. Gerontol. 11 (3) (1956) 298–300.
[16] F.L. Muller, M.S. Lustgarten, Y. Jang, A. Richardson, H. Van Remmen, Free Radic. Biol. Med. 43 (4) (2007) 477–503.
[17] A.V. Razumov, V.A. Likhoshvai, E.A. Ananko, N.V. Vladimirov, K.V. Gunbina, S.A. Lachine, E.A. Nedosekin, S. Nikolaev, L.V. Omelyanchuk, J.G. Matushkin, N.A. Kolchanov, Messenger VOGiS 9 (2) (2005).
[18] V.N. Karnaukhov, Fluorimetric Analysis of Cells, Pushchino, 2002.
[19] V.E. Prokopiev, Biophysical mechanisms of the impact of low-intensity laser radiation on biological tissue and optical methods of diagnosis of their condition. Diss dock. Phys. Math. Sci., Tomsk, 2004.
[20] D.E. Godar, UVA1 radiation triggers two different final apoptotic pathways, J. Invest. Dermatol. 112 (3–12) (1999).
[21] F. Breuckmann, K. Hoffmann, et al., Mechanisms of apoptosis: UVA1-induced immediate and UVB-induced delayed apoptosis in human T cells in vitro, J. Eur. Acad. Dermatol. Venereol. 17 (July (4)) (2003) 418–429.